Fourier transform emission spectroscopy of the jet-cooled CCN free radical

N. Oliphant, A. Lee, and P. F. Bernath

Department of Chemistry, University of Arizona, Tucson, Arizona 85721

C. R. Brazier

Astronautics Laboratory/LSX, Edwards Air Force Base, California 93523

(Received 6 October 1989; accepted 7 November 1989)

The $\widetilde{A}^2\Delta-\widetilde{X}^2\Pi$ electronic transition of the CCN free radical was observed in emission with a high-resolution Fourier transform spectrometer. The CCN was jet-cooled in a corona-excited supersonic jet expansion of diazoacetonitrile (HC(N₂)CN) in helium. From the 000–000, 000–001, 000–002, and 000–100 vibronic bands spectroscopic constants were derived including the ground-state vibrational frequencies, $v_3=1050.7636(6)$, $2v_3=2094.8157(18)$, and $v_1=1923.2547(69)$ cm⁻¹.

I. INTRODUCTION

The CCN radical was first observed in absorption by the flash photolysis of diazoacetonitrile, HC(N₂)CN, by Merer and Travis¹ in 1965. In this study the $\widetilde{A}^2\Delta - \widetilde{X}^2\Pi$, $\widetilde{B}^2\Sigma^- - \widetilde{X}^2\Pi$, and $\widetilde{C}^2\Sigma^+ - \widetilde{X}^2\Pi$ electronic transitions of this linear free radical were analyzed. Using dye laser techniques, Kakimoto and Kasuya² obtained improved constants for the 000–000 band of the $\widetilde{A}^2\Delta - \widetilde{X}^2\Pi$ system and this analysis was subsequently extended to the 010–010 and 020–020 sequence bands.³

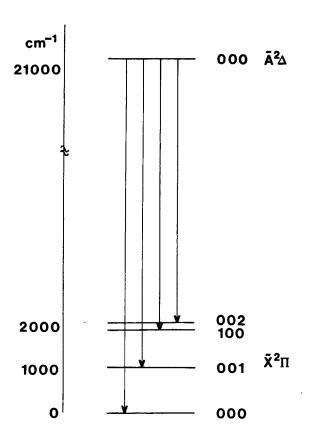
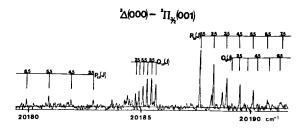


FIG. 1. Energy level diagram showing the $000 \rightarrow 000$, $000 \rightarrow 001$, $000 \rightarrow 100$, and $000 \rightarrow 002$ vibronic emission bands of the $\widetilde{A}^2 \Delta - \widetilde{X}^2 \Pi$ electronic transition of CCN. The very precise wave number scale of the Fourier transform spectrometer allows the ground-state vibrational frequencies v_3 , $2v_3$, and v_1 to be determined.

Microwave-optical double resonances were observed in the excited $\tilde{A}^2\Delta$ state of CCN by Suzuki *et al.*⁴ They were unable to observe ground-state microwave resonances because the dipole moment of the $\tilde{X}^2\Pi$ state is small (0.6D).⁵

Ground-state vibrational frequencies were obtained for the first time by Bondybey and English⁶ in a matrix isolation experiment. More accurate values were determined by dispersing the $\tilde{A}^2\Delta - \tilde{X}^2\Pi$ laser-induced fluorescence with a small monochromator. These and subsequent experiments showed that the original results exhibited an abnormally large matrix shift. More recently, this laser-induced fluorescence was studied at Doppler-limited resolution with a Fourier transform spectrometer. Brazier et al. obtained improved estimates for the Renner-Teller parameters and the ground-state vibrational frequencies. The vibrational frequencies obtained were with one quantum of the bending mode excited and thus the ground-state stretching fun-



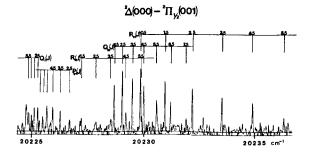


FIG. 2. The $\widetilde{A}^2\Delta - \widetilde{X}^2\Pi_{3/2}$ 000 \rightarrow 001 (upper panel) and $\widetilde{A}^2\Delta - \widetilde{X}^2\Pi_{1/2}$ 000 \rightarrow 001 (lower panel) vibronic subbands of CCN. The rotational structure is indictaed with leader lines.

TABLE I. Line positions for the observed $\tilde{A}^2\Delta - \tilde{X}^2\Pi$ transition of CCN in cm⁻¹. The observed–calculated line positions using the constants of Table II are reported in parentheses.

$CCN \widetilde{A}^2 \Delta - \widetilde{X}^2 \Pi 000-001$							
J	P_1	Q_1	$^{\mathcal{Q}}P_{21}$	R_1			
1.5				20 227.220(14)			
2.5		20 225.259(10)	20 226.690(4)	20 227.861(11)			
3.5		20 225.107(0)	20 226.264(1)	20 228.502(1)			
1.5	20 221.583(1)	20 224.979(2)	$20\ 225.926(-3)$	$20\ 229.170(-6)$			
5.5	$20\ 220.665(-3)$	$20\ 224.865(-3)$	20 225.667(- 6)	20 229.889(9)			
5.5	20 219.778(2)	$20\ 224.784(-4)$	20 225.483(0)	$20\ 230.616(-1)$			
7.5	20218.909(-5)	$20\ 224.740(-2)$	$20\ 225.336(-17)$,			
J	$^{R}Q_{21}$	^S R ₂₁	o _{P12}	$^{P}Q_{12}$			
.5	20 228.648(- 4)	20 230.961(- 2)					
5	20 229.005(1)	20 232.200(4)		$20\ 185.679(-2)$			
3.5	20 229.456(1)	$20\ 233.505(-2)$	20 182.887(4)	20 185.485(2)			
.5	20 229.982(1)	20 234.884(1)	20 181.885(- 1)	20 185.280(- 1)			
.5	20 230.576(1)	20 236.323(4)	20 180.882(- 3)	20 185.086(3)			
.5	20 231.230(3)	20 237.813(5)	20 179.888(- 1)	20 184.902(2)			
.5	20 231.934(1)	20 239.316(- 34)	20 178.896(- 10)	20 184.736(1)			
.5	20 232.685(- 6)	20 240.944(5)	201,0.000(10)	20 184.583(- 7)			
.5	20 202.003(- 0)	20 2 1012 FT(2)		20 184.467(- 2)			
J	P_2	$^{Q}R_{12}$	Q_2	R_2			
.5		20 187.679(0)	20 189.124(1)				
.5 .5		20 187.879(0)	20 189.124(1) 20 189.424(- 13)	20 192.639(11)			
.5 .5				20 192.839(11)			
		20 188.877(- 1)	20 189.832(2)	• •			
.5		20 189.479(- 1)	20 190.283(- 3)	20 195.184(- 3)			
.5		20 190.098(2)	20 190.797(6)	20 196.556(21)			
.5		20 190.739(10)	20 191.300(39)	20 197.914(- 7)			
.5		$20\ 191.362(-21)$	20 191.904(- 22)	20 199.337(- 5)			
.5		20 192.061(0)	20 192.560(11)				
0.5		20 192.776(14)	20 193.192(- 13)				
	P 0	CCN $\tilde{A}^2\Delta - \tilde{X}^2\Pi$ 000-	002	P 0			
J	^R Q ₂₁	Q ₁	Q P ₂₁	^P Q ₁₂			
5		$19\ 181.117(-24)$	$19\ 182.548(-1)$	$19\ 141.721(-2)$			
.5	$19\ 185.361(-3)$	19 181.024(3)	19 182.174(2)	19 141.545(1)			
.5	19 185.916(4)	19 180.941(33)	19 181.857(4)	19 141.366(3)			
.5	19 186.531(- 1)	19 180.834(9)	19 181.627(- 5)	19 141.193(0)			
.5		19 180.774(- 3)	$19\ 181.446(-26)$	$19\ 141.037(-5)$			
.5				$19\ 140.913(-1)$			
J	$^{Q}R_{12}$	Q_2	R_2 .				
.5	19 143.709(0)		19 147.443(- 23)				
.5	$19\ 144.322(-1)$		19 148.682(11)				
.5	19 144.941(4)		19 149.956(14)				
.5	19 145.561(- 1)	19 146.362(6)	19 151.270(0)				
.5	19 146.200(- 5)	19 146.895(- 6)	19 152.654(1)				
5.5	19 146.859(- 12)	19 147.475(6)	• •				
.5	19 147.555(- 7)	19 148.099(- 7)					
	, ,						
J	$^R\mathcal{Q}_{21}$	$\stackrel{CCN}{\stackrel{\sim}{a}}\stackrel{\sim}{A}^2\Delta -\stackrel{\sim}{X}^2\Pi 000-$	∘100 ^Q P ₂₁	$^{P}Q_{12}$			
-	€21	- 12	* ZI	\$ 12			
.5	19 356.190(23)	19 315.186(3)		10.010.1017			
5	$19\ 356.492(\ -30)$	19 315.792(6)	10.252.500.453	19 313.181(- 5)			
.5	$19\ 356.971(-3)$	19 316.386(1)	19 353.799(17)	19 312.981(10)			
1.5	19 357.513(9)	19 317.613(3)	19 353.466(14)	19 312.791(- 1) 19 312.610(12)			
5.5	$19\ 358.074(-26)$						

damentals were known only to ± 10 cm⁻¹.

In the present work we used a corona-excited supersonic jet source¹⁰ to observe the cold emission spectrum of the $\tilde{A}^2\Delta - \tilde{X}^2\Pi$ transition of CCN. The emission from the 000–

000, 000–001, 000–002, and 000–100 vibronic bands were recorded using a high-resolution Fourier transform spectrometer. This has provided much improved estimates for the ν_1 , ν_3 and $2\nu_3$ vibrational frequencies of the $\widetilde{X}^2\Pi$ state.

II. EXPERIMENTAL

Cold molecular emission from the CCN radical was produced via a corona-excited supersonic expansion. 10 A potential of 3 kV was provided by a high-voltage power supply through a ballast resistor of 2 M Ω to a 250 μ m diameter tungsten wire. The tungsten wire ends 400 μ m from a 250 μ diameter pinhole nozzle.

Small amounts of the precursor diazoacetonitrile were added by flowing helium over the sample which was maintained in an ice bath at 0 °C. The diazoacetonitrile was synthesized by following the procedure of Dewar and Petit.¹¹ The ether solution was concentrated by flowing N₂ over the sample while it was maintained at a temperature of -18 °C. The residual ether was evaporated in situ just prior to use. When all of the ether was gone, the intensity of OH A-Xemission dropped sharply. The backing pressure of the carrier gas was 4 atm, while a 250 cfm Roots blower maintained a pressure of several hundred millitorr in the vacuum chamber.

The potential drop through the nozzle provided the electrical excitation to form a plasma. The subsequent expansion collisionally cooled the rotational temperature to about 30 K. The electronic emission of the rotationally cooled molecules was observed by focusing the emission perpendicular to the molecular jet onto the entrance aperture of the McMath Fourier transform spectrometer of the National Solar Observatory at Kitt Peak.

A total of four scans were recorded in 18 min of integration at a resolution of 0.025 cm⁻¹. A red pass color filter and a blue pass interference filter limited the wavelength region to 430-600 nm. The detectors were two cooled GaAs RCA C31034 photomultiplier tubes.

III. OBSERVATIONS AND ANALYSIS

The interferogram was transformed by G. Ladd of the National Solar Observatory to yield the spectrum. The emission spectrum was found to contain the 000-000, 000-001, 000–002, and 000–100 vibronic bands (Fig. 1) of the $\tilde{A}^2\Delta$ – $\tilde{X}^2\Pi$ transition of CCN. The 000 - 020 band was not present. Additional features could be assigned to the $A^3\Pi_{e}$ $X^3\Pi_u$ Swan system¹² of C_2 and numerous highly vibrationally excited bands of the $A^{2}\Pi - X^{2}\Sigma^{+}$ red^{12,13} system of CN.

The four vibronic subbands were measured with the data reduction program PC-DECOMP developed at the National Solar Observatory. Each line was fitted using a Voigt line shape function. The observed lines were Gaussian with a

width of approximately 0.045 cm⁻¹ comparable to the room temperature Doppler linewidth of 0.041 cm⁻¹. Clearly the jet provides rotational cooling (Fig. 2), but because the entire free jet was imaged through the entrance aperture of the spectrometer, there was no reduction in linewidth.

The line positions were easily assigned with the help of the previous vibrational and rotational constants. Our measured line positions for the 000–000 $\tilde{A}^2\Delta - \tilde{X}^2\Pi$ agree, within experimental error, with the previous more extensive measurements of Kakimoto and Kasuya.² We, therefore, fixed the spectroscopic constants for this band to their values. For convenience we used the same Hamiltonian and matrix elements for the $\tilde{A}^2\Delta$ and $\tilde{X}^2\Pi$ states of CCN as Kakimoto and Kasuva.

The line positions of the 000-001, 000-002, and 000-100 vibronic bands are reported in Table I. The best signalto-noise ratio is about 15, so these line positions have a maximum precision (and accuracy) of about 0.003 cm⁻¹. Typically the signal-to-noise ratio is closer to 5 so the majority of the data has a precision of about 0.01 cm⁻¹. The line positions of Table I were reduced to the molecular constants of Table II. The Λ -doubling constants, p and q, could not be determined and were set to zero for the $\bar{X}^2\Pi$ vibronic states. Since the jet is rotationally cold, the centrifugal distortion constants D were also not determined but were constrained to the $\tilde{X}^2\Pi$ 000 value² of 2.206 \times 10⁻⁷ cm⁻¹. The spin-rotation parameter γ for the 001 state was barely determined, the other γ 's were set to the $\tilde{X}^2\Pi$ 000 value² of -37.57×10^{-4} cm^{-1}

IV. DISCUSSION

Electronic emission spectroscopy is generally much more sensitive than infrared absorption spectroscopy because electronic transition dipole moments are usually larger than infrared vibration-rotation transition moments. In addition, emission spectroscopy is a zero background technique which has no noise from the absorption continuum required for absorption measurements. Unfortunately, the electronic emission spectra of polyatomic molecules are usually very dense and complex. This complex structure can be simplified by cooling in a free jet expansion or by selective excitation with a laser (for example, Ref. 9).

In our experiments we exploit the very accurate wave number scale of a Fourier transform spectrometer to determine the fundamental vibrational frequencies of CCN (Table II). Our measurements are comparable in accuracy to

TABLE II. Molecular constants for the $\tilde{A}^2\Delta - \tilde{X}^2\Pi$ transition of CCN (in cm⁻¹). One standard deviation error is reported in parentheses.

Constant	$\tilde{X}^2\Pi(001)$	$\tilde{X}^2\Pi(002)$	$\tilde{X}^2\Pi(100)$	
ν_0	1050.763 6(6)	2094.815 7(18)	1923.254 7(69)	
3	0.395 661(17)	0.393 233(59)	0.395 35(38)	
4 _{eff}	40.295 2(12)	40.140 2(29)	40.306 9(79)	
$A_{\rm eff} \times 10^4$	- 59(27)	− 37.57 ^b	- 37.57 ^b	
$D \times 10^7$	2.206 ^b	2.206 ^b	2.206^{b}	

The molecular constants for the $v = 0 \tilde{A}^2 \Delta$ state were held fixed to the values in Ref. 2. The T_{00} for the 000–000 band is 21 259.203 14 cm⁻¹.

^b Fixed to the value for the $\tilde{X}^2\Pi$ 000 (Ref. 2).

TABLE III. Harmonic frequencies^a and anharmonic corrections for the $\tilde{X}^2\Pi$ state of CCN (in cm⁻¹).^b

$\omega_1 = 1930.744(14)$	$x_{12} = -7.4889(82)$
$\omega_2 = 324.0$	$x_{23} = 11.5361(37)$
$\omega_3 = 1045.9390(58)$	$x_{33} = -2.6000(24)$
	$y_{233} = -0.7558(15)$

^a Values in parentheses are one standard deviation statistical error estimates.

the values which would be obtained in a direct infrared absorption measurement.

Note that the bending mode of CCN (near 324 cm⁻¹) remains to be measured accurately. The 000–010 $\widetilde{A}^2\Delta - \widetilde{X}^2\Pi$ transition is only vibronically allowed, while 000–020 band has (apparently) a small Franck–Condon factor. Perhaps a direct far infrared measurement would be the best method for determining ν_2 for CCN.

The fundamental vibrational frequencies determined here are somewhat different from the values in our earlier work. This is due to the presence of significant x_{12} and x_{23} anharmonic contributions. Combining all the available data produces the harmonic frequencies and anharmonic corrections given in Table III. It should be noted that several anharmonic corrections are still not known.

The $\rm CN^{14}$ and $\rm C_3N^{15}$ molecules have been found in interstellar clouds and in stellar envelopes by microwave spectroscopy. Unfortunately, the accidentally small dipole moment⁵ of CCN has inhibited microwave detection. With the vibrational constants reported here we plan to make an infrared search for CCN in the carbon star IRC + 10216. The CCN molecule is also important in $\rm HCN + NO_2$ and

 $(CN)_2 + NO_2$ flames and in the combustion of energetic materials in general. ¹⁶

ACKNOWLEDGMENTS

The National Solar Observatory is operated by the Association of Universities for Research in Astronomy, Inc., under contract with the National Science Foundation. We thank J. Wagner, G. Ladd, and P. Carrick for assistance in acquiring our spectrum. Acknowledgment is made to the donors of the Petroleum Research Fund, administered by the American Chemical Society, for partial support of this work. Support was also provided by the Astronautics Laboratory, Edwards AFB, Grant F04611-87-K-0020.

¹A. J. Merer and D. N. Travis, Can. J. Phys. 43, 1795 (1965).

^bData from this work and Ref. 9.

²M. Kakimoto and T. Kasuya, J. Mol. Spectrosc. 94, 380 (1980).

³K. Kawaguchi, T. Suzuki, S. Saito, E. Hirota, and T. Kasuya, J. Mol. Spectrosc. 106, 320 (1984).

⁴T. Suzuki, S. Saito, and E. Hirota, J. Chem. Phys. 83, 6154 (1985).

⁵K. Yamashita and K. Morokuma, Chem. Phys. Lett. 140, 345 (1987).

⁶V. E. Bondybey and J. H. English, J. Mol. Spectrosc. 70, 236 (1978).

⁷K. Hakuta and H. Uehara, J. Chem. Phys. 78, 6484 (1983).

⁸K. Hakuta, H. Uehara, K. Kawaguchi, T. Suzuki, and T. Kasuya, J. Chem. Phys. 79, 1094 (1983).

⁹C. R. Brazier, L. C. O'Brien, and P. F. Bernath, J. Chem. Phys. 86, 3078 (1987).

¹⁰P. C. Engelking, Rev. Sci. Instrum. 57, 2274 (1986).

¹¹M. J. S. Dewar and R. Petit, J. Chem. Soc. 1965, 2026.

¹²R. W. B. Pearse and A. G. Gaydon, *The Identification of Molecular Spectra*, 4th ed. (Chapman Hall, London, 1976).

¹³F. J. LeBlanc, J. Chem. Phys. 48, 1980 (1968).

¹⁴R. L. Dickman, W. B. Somerville, D. C. B. Whittet, D. McNally, and J. C. Blades, Astrophy. J. Suppl. 53, 55 (1983).

¹⁵M. Guélin and P. Thaddeus, Astrophys. J. Lett. 212, L81 (1977).

¹⁶L. Thorne (personal communication); O. I. Smith and L. R. Thorne, "Structure of Cyanogen-Nitrogen Dioxide Premixed Flames," Paper WFS/CI86-34 presented at the Fall Meeting of the Western States Section of the Combustion Institute, Tucson, Arizona, October, 1986.